Investigation of Thermal Stability of Red Emitting SrGd$_{2(1-x)}$Eu$_{2x}$O$_4$ Phosphors for Lighting and Display Applications

Jyoti Singh*, J. Manam, Puja Kumari, Subhajit Jana

Department of Applied Physics, Indian Institute of Technology (Indian School of Mines) Dhanbad

Novel red-emitting SrGd$_{2(1-x)}$Eu$_{2x}$O$_4$ samples were prepared via combustion method. Structural and optical characteristics were examined with the help of XRD, FTIR, FESEM and photoluminescence (PL) studies. FESEM images reveal agglomerated rod-like morphology. The intense red emission corresponding to $^5D_0{\rightarrow}^7F_2$ transitions under UV-excitation 276 nm and higher thermal stability up to 250 °C of SrGd$_{2(1-x)}$Eu$_{2x}$O$_4$ reveals its applicability in lighting and display devices.

Keywords: Phosphors, Photoluminescence, Thermal stability.

1. INTRODUCTION

Nowadays, rare-earth (RE) doped binary oxides having general formula ARE$_2$O$_4$ (where, A = Sr, RE = Gd) materials are receiving the attention of scientific communities because these materials show high density (7.3 gm/cm^3), good charge stability and high physical and chemical robustness [1-14]. Furthermore, the same valence state and similar ionic radii of Gd^{3+} provides an easier way for incorporation of luminescent centers such as Eu^{3+}, Dy^{3+}, Tb^{3+} etc. Above mentioned characteristics of these host reveals its extensive applications towards the development of display devices such as field-emission displays (FED), plasma display panels (PDP) and white light-emitting diodes (W-LED) [1-3].

In this context, Eu^{3+} doped SrGd$_2$O$_4$ has chosen as a host lattice synthesized by combustion method and Eu^{3+} ions used as a dopant in order to yield strong red emissions. The structural and optical properties of prepared phosphors are measured by XRD, FESEM, and PL characterizations. The XRD results revealed the appearance of orthorhombic SrGd$_2$O$_4$ phase with space group Pnam (62). The photoluminescence (PL) excitation and emission spectra show the characteristic emission peaks of Eu^{3+} due to its presence in the host-lattice. The most intense peaks of Eu^{3+} were obtained at 615 nm and 595 nm which correspond to $^5D_0{\rightarrow}^7F_2$ and $^7F_1$ transition, respectively. Photometric characterization and thermal stability of phosphors were determined by temperature dependent PL and Arrhenius fit. The present samples show all the characteristics of a suitable phosphor material for display and lighting application.

2. EXPERIMENTAL

High purity [Sr(NO$_3$)$_2$], [Gd(NO$_3$)$_3$] and [Eu(NO$_3$)$_3$] is taken 1:2$_{(1-x)}$:2$_x$ molar ratio in a beaker. Urea [H$_2$NCONH$_2$] is used as a fuel and its amount is calculated using total oxidizing and reducing valences. All these chemicals are taken in a beaker and mixed in deionised water.

An aqueous concentrated paste containing a calculated amount of metal nitrates and urea in preheated furnace maintained at 500 °C, white foamy solid obtained by combustion process. The solid obtained was again fired at 1200 °C for 5 h to increase the brightness and crystallinity.

The crystalline structure of prepared materials, morphology of particles and their optical properties were examined by XRD, FTIR, FE-SEM and photoluminescence studies (PL). The X-ray diffraction (XRD) patterns of the phosphors prepared at various temperatures were recorded on Bruker-D8 Focus X-ray powder diffractometer with Cu K_α = 1.5406 Å. The morphology of prepared phosphors was examined by the field-emission scanning electron microscope (FESEM Supra-55, Germany) images. The room-temperature photoluminescence (PL) excitation, emission spectra and life time measurement were recorded on Horiba FL3-21 fluorescence spectrophotometer. The temperature-dependent PL was performed with Cary Eclipse Fluorescence spectrophotometer comprising of a Xenon lamp as an excitation source and a temperature-controlled square-shaped brass block. The temperature of the brass block is controlled and maintained by a proportional-integral-derivative (PID) controller and a *K*-type thermocouple.

3. RESULTS AND DISCUSSIONS

The XRD patterns of prepared at 1200 °C show the orthorhombic phase with space group Pnam (Fig. 1). However, an insignificance presence of impurity phase cubic Gd$_2$O$_3$ having JCPDS No. 076-0155 is also observed. The lattice parameters of the unit cell are a = 10.095 Å, b = 12.009 Å and c = 3.4603 Å which are in correspondence with the JCPDS database for SrGd$_2$O$_4$ (JCPDS No. 052-1744).

It can be seen in Fig. 1 that all the samples having different Eu^{3+} contents show same XRD profile and there is absence of impurity phases associated to europium. XRD results reveal that Eu^{3+} doping does not alter the basic crystal structure of the host lattice and properly incorporated in the host lattice.
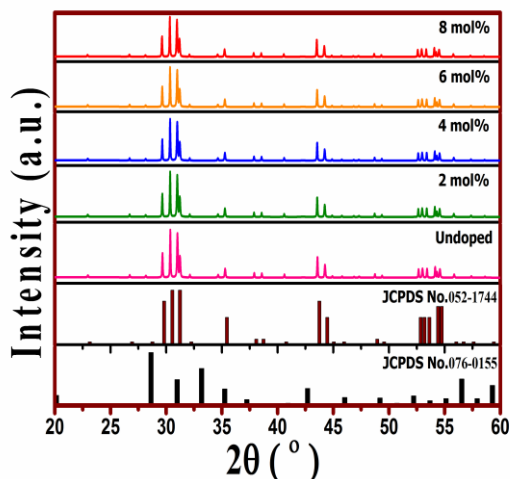
* jyoti.singh.phy@gmail.com

Fig. 1 – XRD studies of $SrGd_{2(1-x)}Eu_{2x}O_4$ samples

In order to find out the crystallite size of Eu^{3+} activated $SrGd_2O_4$ samples, Debye-Scherrer method and Hall-Williamson relations are adopted. The average crystallite sizes of Eu^{3+} doped $SrGd_2O_4$ powder samples were calculated by the Debye Scherrer method which is given by the formula:

$$D = \frac{0.9\lambda}{\beta\cos\theta}$$

where, β is full width at half maxima (FWHM) and D is the crystallite size.

In order to verify the crystallite sizes obtained from Debye-Scherrer method, the crystallite sizes were also calculated from Hall-Williamson relation, which is given by the equation:

$$\frac{\beta\cos\theta}{\lambda} = \frac{1}{D} + \frac{\varepsilon\sin\theta}{\lambda}$$

where ε is the micro-strain present in the sample.

Fig. 2 shows the Hall–Williamson plot of the XRD graphs for Eu^{3+} doped $SrGd_2O_4$. The crystallite sizes and the calculated micro-strain are shown in Table 1. The crystallite sizes of all the samples are found to be in the range of 15 - 65 nm. Table 1 shows a systematic reduction in the crystallite size of the $SrGd_2O_4$:Eu^{3+} samples with an increase in the doping concentrations (1-8 mol %), which suggest that the incorporation of Eu^{3+} ions suppresses the growth of the crystals.

FTIR studies were performed in the range 400 - 4000 cm^{-1} of prepared samples to examine the detailed structure of the bonding environment. Fig. 3 shows the FTIR spectrum of Eu^{3+} doped $SrGd_2O_4$ samples. The important structural entities associated with the vibrations of Gd-O and Sr-O bonds are seen in the range of 540 to 592 cm^{-1}, respectively [3, 4]. The broad transmission minima at 1458 cm^{-1} can be attributed to -CH_3 bending mode. However, two relatively low intense peaks, situated at 859 and 1380 cm^{-1} are designated to be the stretching and bending modes of C-H bond, respectively. It is worth to mention that the presence of residual contents such as C = N, C-H and O-H vibrations has a negative effect on the photoluminescence
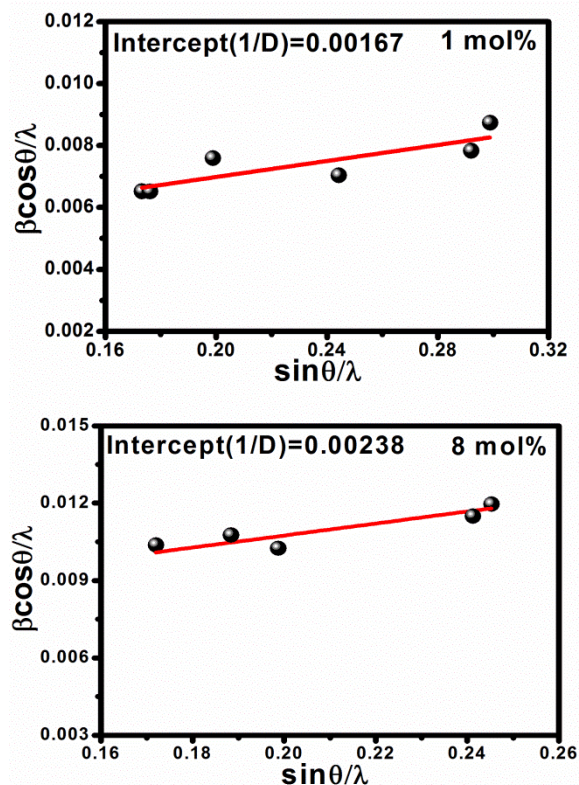

Fig. 2 – Hall-Williamson plots of Eu^{3+} doped $SrGd_2O_4$ phosphors

since these defects on the surface of particles act as a source of quencher on luminescence intensity [4]. In the present case, the less intense peaks of residue contents suggest the high phase purity of $SrGd_2O_4$ matrices which are able to enhance the photoluminescence efficiency. The FTIR spectra show that the particles are free from any organic radical and fit for the PL studies.

Table 1 – Crystallite size distribution and microstrain of Eu^{3+} doped $SrGd_2O_4$ phosphors

Compounds $SrGd_2O_4$:Eu^{3+}	Debye-Scherrer	Hall-Williamson	Microstrain ε ($\cdot 10^{-3}$)
1 mol%	10-55	50	20
2 mol%	15-55	44.5	18.6
4 mol%	15-55	40.8	18
6 mol%	15-55	36.4	12
8 mol%	15-55	32.0	10.5

Fig. 4 shows the field emission scanning electron microscope (FESEM) images of Eu^{3+} doped SrGd2O4 samples prepared at 1200 °C. It is remarkable that all the samples are exhibiting agglomerated rod-shaped morphology having sizes with an average length of about 0.3-3 μm. All the samples show similar morphology which indicates that the doping of Eu^{3+} ions do not affect the morphology of samples.

Additionally, it is noteworthy that many pores and voids are also present in these FESEM images. The presence of pores and voids is owing to the fact that, in the combustion process the reaction takes place in a very short duration of time with the evolution of a lot of gases that generally generates nanosized materials
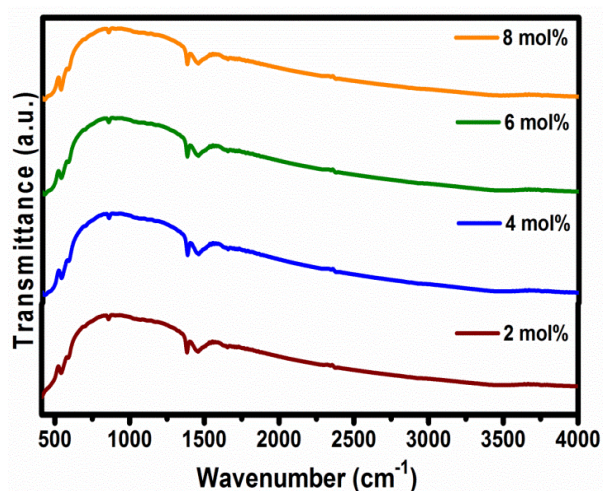
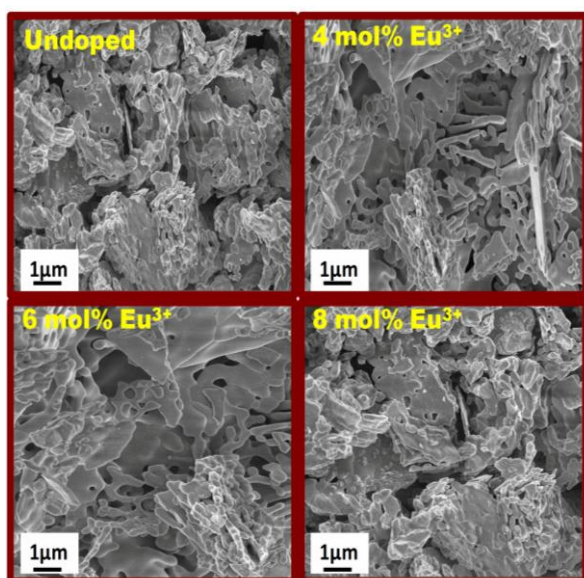**Fig. 3** – Room temperature FTIR spectra of Eu^{3+} doped $SrGd_2O_4$ phosphors

Fig. 4 – FESEM studies of $SrGd_{2(1-x)}Eu_{2x}O_4$ samples

with pores and voids [3, 4]

It is found that the crystallite sizes of all the samples obtained from Hall-Williamson and Debye-Scherrer method are found to be in the range of 30-50 nm which is much less than the particle sizes obtained from FESEM images. The reason behind this is because the particle shows clustered form of many single crystals [5].

Fig. 5a-b shows the room temperature photoluminescence excitation and emission spectra of as-synthesized $SrGd_{2(1-x)}Eu_{2x}O_4$ samples. All the transitions of excitation and emission spectra are assigned and shown in Fig. 5a-b. The PL excitation and emission spectra of Eu^{3+} activated $SrGd_2O_4$ phosphors were recorded and the emission wavelengths fixed at 615 nm while the excitation wavelength at 276 nm, respectively [3, 4].

The emission spectra contained six distinct emission peaks centered around 582, 594, 615, 627, 656 and 711 nm are associated to 4f transitions of Eu^{3+} from the upper excited level $^5D_0$ to lower ^7F_j ($j = 0, 1, 2, 3$ and 4)

levels respectively (Fig. 5b). The strongest emission band at 615 nm and the weakest one at 627 nm are attributed to the electric dipole transition $^5D_0\rightarrow^7F_2$, which is hypersensitive in the host structure symmetry.

Generally, the PL intensity of the phosphors relies on the doping concentration. It is expected that with the increase of doping concentrations photoluminescence should increase. However, the PL intensity decreases after 4 mol% Eu ions due to the non-radiative interaction between the ions as the resonant energy transfer becomes stronger rather than by emission of visible light, called concentration quenching (Fig. 5b-c) [2-4].
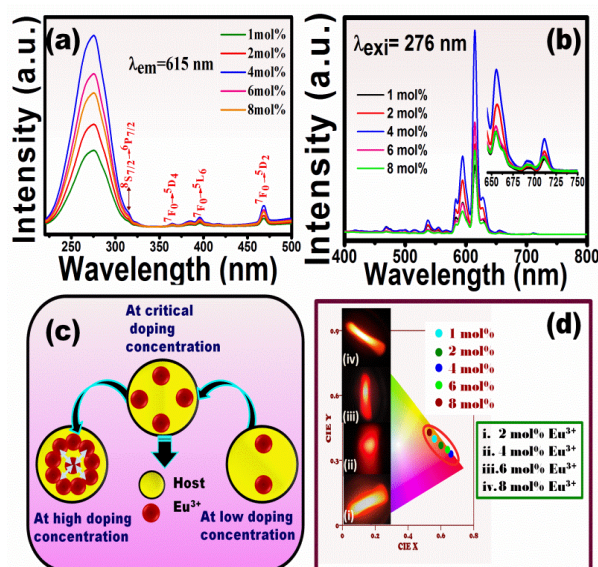

Fig. 5 – (a) PL excitation spectra, (b) PL emission spectra of $SrGd_{2(1-x)}Eu_{2x}O_4$ samples, (c) representation of quenching phenomenon, (d) CIE diagram with digital images of phosphors excited with 276 nm UV light

Fig. 5d illustrates the CIE (Commission Internationale de l'Eclairage) chromaticity diagram of $SrGd_2O_4$:Eu^{3+} phosphors for different Eu^{3+} concentrations. The colour coordinates (0.66, 0.33) corresponding to the red emission were observed for 4 mol% concentration of Eu^{3+}, which is very much nearer to the commercial red phosphor Y_2O_2S:Eu^{3+} (0.67, 0.33) [4]. The following results suggest that $SrGd_2O_4$:Eu^{3+} phosphors are suitable for lighting and display applications.

The temperature stability of the phosphors is the key factors when the practicle applicability is taken into account. To investigate the effect of temperature on luminescence of the synthesized phosphors, the emission spectra of 4 mol% Eu^{3+} doped $SrGd_2O_4$ samples at 276 nm excitation were measured at different temperatures ranging from 300 to 523 K (Fig. 6). Similar spectral profiles are observed for all the samples having different Eu^{3+} contents.

It is clearly visible in Fig. 6 that the emission intensity of the samples was decreased with the increase in the sample temperature. But, the integrated emission intensity of Eu^{3+} ions remained more than 80% at 523 K of those recorded at room temperatures, as shown in Fig. 6.
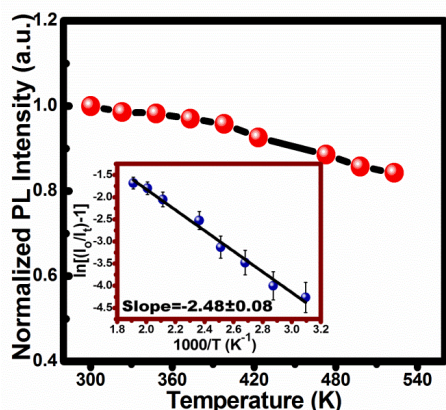
Fig. 6 – Temperature dependent PL and Arrhenius plot of $SrGd_{1.92}Eu_{0.08}O_4$ samples

The activation energy (ΔE) for thermal quenching can be obtained by using Arrhenius fit. The Arrhenius fitting of the emission intensity of $SrGd_2O_4{:}Eu^{3+}$ samples were investigated and given in the inset of Fig. 6. The activation energy (ΔE) can be expressed by the following equations [10, 11]:

$$I_t = \frac{I_0}{1+c\exp\left(-\dfrac{\Delta E}{kT}\right)}$$

where, I_0 and I_t are the luminescence intensities at room and testing temperatures respectively, c is a constant and k is the Boltzmann constant ($8.617 \cdot 10^{-5}$ eV·K^{-1}).

The fitting of $\ln(I_0/I_t - 1)$ vs. 1000/T gives the estimation of activation energy (ΔE) for the present phosphor (inset of Fig. 6). It is estimated to be 0.21 eV for the Eu^{3+} doped $SrGd_2O_4$ phosphors. The thermal stable behaviour of present phosphor system is found to be more than the commercial red phosphor $Y_2O_3{:}Eu^{3+}$ and $Y_2O_2S{:}Eu^{3+}$, respectively [10-14]. The above results validate the suitability of present host for advanced lighting and color display devices.

To clarify the physical mechanism behind temperature quenching, it is important to explain the crossover process (Fig. 7). The crossover process has been widely observed in various Eu^{3+} activated host matrices [22, 23]. The typical configurational coordinate representation of the crossover process from $^5D_0$ level to the Eu-O charge transfer band (CTB) is shown in the Fig. 7. In this process, the electron

situated at $^5D_0$ state can be thermally activated and goes to the CTB through the cross point and then further relaxes through another cross point of CTB to ^7F_J states, finally tending towards the ground state of Eu^{3+}. In this process, the electron absorbs the thermal energy to overcome the potentialbarrier (ΔE) also called the activation energy [10, 11].

The value of the activation energy mainly relies on the location of the $O^{2-}{\to}Eu^{3+}$ CTB, since the position of the $^5D_0$ level is almost independent from host matrices. Higher activation energy may arise due to higher location of CTB. It is easy to understand that the higher the activation energy is, the harder the crossover is and the most thermally stable the phosphor is [10, 11]. Moreover, the complex crystal structure of the present phosphor system could also be a reason of high thermal stability of the $SrGd_2O_4$ phosphors.
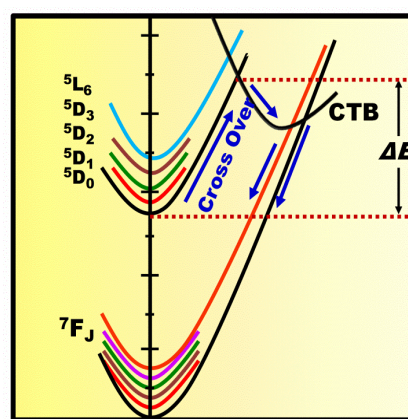

Fig. 7 – Configurational coordinate diagram of thermal quenching mechanism

In addition, the relatively high activation energy of Eu^{3+} doped $SrGd_2O_4$ samples compared to the commercially used red phosphor $Y_2O_2S{:}Eu^{3+}$ indicating that the present phosphor has a good thermal stability and could be applied for high-powered lighting and display applications.

AKNOWLEDGEMENTS

REFERENCES

1. C.R. Ronda, T. Jüstel, H. Nikol, *J. Alloys Compd.* **275–277,** 669 (1998).
2. B. Marí, K.C Singh, M. Sahal, S.P. Khatkar, V.B. Taxak, Mukesh Kumar, *J. Lumin.* **131,** 587 (2011).
3. Jyoti Singh, Pankaj Kr. Baitha, J. Manam, *J. Rare Earths* **33,** 1040 (2015).
4. Jyoti Singh, J. Manam, *J. Mater. Sci.* **51,** 2886 (2016).
5. Partha P. Pal, Jairam Manam, *Mat. Sci. Eng. B* **178**, 400 (2013).
6. S. Arul Antony, K.S. Nagaraja, G.L.N. Reddy, O.M. Sreedharan, *Mater. Lett.* **51**, 414 (2001).
7. G. Seeta Rama Raju, Jae Su Yu, *Spectrochim. Acta A* **124**, 383 (2014).
8. Liya Zhou, Jianxin Shi, Menglian Gong, *J. Phys. Chem. Solids* **68**, 1471 (2007).
9. N. Lakshminarasimhan, U.V. Varadaraju, *J. Solid State Chem.* **181**, 2418 (2008).
10. Yue Tian, Baojiu Chen, Ruinian Hua, Naisen Yu, Baoquan Liu, Jiashi Sun, Lihong Cheng, Haiyang Zhong, Xiangping Li, Jinsu Zhang, Bining Tian, Hua Zhong, *Cryst. Eng. Comm.* **14,** 1760 (2012).
11. Maheshwary, B.P. Singh, R.A. Singh, *New J. Chem.* **39,** 4494 (2015).
12. Hsin-Cheng Lin, Che-Yuan Yang, Subrata Das and Chung- Hsin Lu, *Ceram. Int.* **40**, 12139 (2014).
13. Subrata Das, Che-Yuan Yang, Hsin-Cheng Lin, Chung-Hsin Lu, *RSC Adv.* **4**, 64956 (2014).
14. Joydip Sengupta, R.K. Sahoo, K.K. Bardhan, C.D. Mukherjee, *Mater. Lett.* **65**, 2572 (2011).